

Kinetics of Abstraction of D and O on Cu(110) Surfaces by Gaseous H Atoms

D. Kolovos-Vellianitis[†] and J. Küppers^{*,†,‡}

Experimentalphysik III, Universität Bayreuth, 95440 Bayreuth, Germany, and Max-Planck-Institut für Plasmaphysik (EURATOM Association), 85748 Garching, Germany

Received: August 21, 2002; In Final Form: November 15, 2002

The kinetics of HD and water formation during admission of H atoms to D- and O-covered Cu(110) surfaces was measured and compared to the kinetics of the analogous reactions on Cu(100), Cu(111), and other metal surfaces. The phenomenology of the HD abstraction kinetics on Cu(100) is according to an Eley-Rideal (ER) mechanism with a cross-section of 2.4 \AA^2 and only a small contribution of D_2 products provides evidence for the operation of a hot-atom mechanism. Similar features were observed on the other Cu surfaces. As origin of the ER-phenomenology on Cu surfaces the inefficiency of electron-hole excitation for hot-atom sticking due to the small density of states at the Fermi level of Cu is proposed. Unlike at Cu(100), the H adsorption-induced reconstruction of the surface does not affect the abstraction kinetics. The interaction of gaseous H with oxygen adsorbed on Cu(100) leads to adsorbed and gaseous water products at 100 K. The occurrence of a considerable fraction of gaseous water at reaction temperatures 60 K below the water desorption temperature indicates that the substantial exothermicity of the reaction leads to energetically ejected product upon their formation. In accordance with other water formation reactions between gaseous H and adsorbed oxygen the mechanism is identified as two sequential hydrogenation reactions, O to adsorbed OH and OH to gaseous and adsorbed water, of which the latter is rate-determining with a cross-section of 0.6 \AA^2 . At reaction temperatures well above the water desorption temperature, isothermal desorption is absent in the water kinetics and only gaseous water was monitored. The coverage of oxygen has no effect on the water kinetics.

1. Introduction

The interaction of gaseous H atoms with adsorbates on solid surfaces can lead to reactions without the H atom being accommodated on the surface prior to reaction. Due to the substantial potential energy of an H atom in front of a surface with a strong H-substrate attraction, such a "direct" reaction can be fairly exothermal and the reaction product might be ejected into the gas phase as an energetic particle which carries the available reaction enthalpy in internal degrees of freedom. The pioneering molecular beam/laser spectroscopy studies of Rettner and Auerbach^{1,2} on abstraction of D(ad) on Cu(111) by H(gas) toward HD(gas) confirmed the expectation drawn from the reaction energy balance and provided a first insight into the dynamics of a direct reaction.

The kinetics of direct reactions were often described in an Eley-Rideal (ER) scenario through a quasi-first-order process controlled by the flux of incoming atoms ϕ , a reaction cross section σ , and the momentary adsorbate coverage Θ . With Θ_0 as the initial coverage of the adsorbate and an atom flux which is switched on at $t = 0$, one obtains as rate $R(t)$ of the ejected gas-phase species $R(t) = \Theta_0 \exp(-\sigma\phi t)$.

The general applicability of the ER mechanism to D(ad) by H(gas) abstraction reactions was questioned by the observation of D_2 (gas) product molecules in a study of D(ad) by H(gas) abstraction on Ni(100) surfaces by Winkler and co-workers.³

Studies of the D(ad) by H(gas) abstraction kinetics on various metal and semiconductor surfaces performed in this laboratory,

e.g., Ni(110),⁴ Pt(111),⁵ Cu(111),⁶ and Si(100),⁷ revealed that the HD rates measured at small initial D(ad) precoverages might substantially contradict the operation of an ER mechanism (Ni, Pt) or be in accordance with it (Cu), possibly in a restricted temperature range (Si). It was observed in these studies that marked deviation from the ER kinetics in the HD rates was accompanied by contributions from D_2 products in the few percent range.

The HD and D_2 kinetics measured on various surfaces were successfully described by random walk⁸ and analytical^{9,10} models assuming that H atoms approaching a substrate from the gas phase get transferred into an energetic not-accommodated mobile hot-atom state¹¹ on the surface. Travelling across the surface in this hot-atom state the H atom might react with adsorbed D or H with a probability p_r , stick at empty sites with probability p_s , or generate hot D with probability p_d upon collisions with an adsorbed D which then assumes the role of a hot atom and proceeds likewise. The random walk and analytical models revealed that the HD and D_2 kinetics and yields are determined by the ratio p_r/p_s and p_d only. Furthermore, the analytical models explained why the HD rates at late reaction times necessarily exhibit an ER-like exponential decay according to the above rate expression. Through variation of p_r/p_s and p_d , excellent qualitative agreement between theoretical and measured HD and D_2 rates was obtained.

The HD kinetics measured in the abstraction reaction of D(ad) on Cu(111) by H(gas) was found as almost perfect ER-like,⁶ conforming to a p_r/p_s ratio of about unity within the above-mentioned models: the HD rate $R(t)$ was a pure exponential. The contribution of D_2 products to the total abstraction yield was small, only about 1%, but their kinetics was of second order with respect to the D coverage, as required from the models.

* Corresponding author. Tel: (+49) 921-553800. Fax: (+49) 921-553802. E-mail: kueppers@uni-bayreuth.de.

[†] Universität Bayreuth.

[‡] Max-Planck-Institut für Plasmaphysik (EURATOM Association).

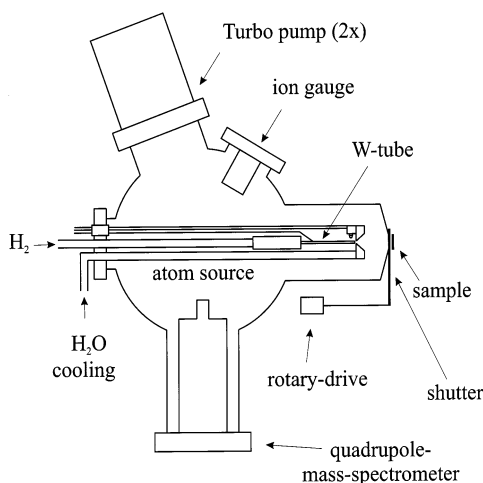


Figure 1. Schematics of the source chamber with integral H atom source and quadrupole mass spectrometer.

In contrast to this, the characteristics of the HD kinetics of the D(ad) abstraction reaction on Cu(100) surfaces could only be explained within the analytical model by assuming that two different cross-sections control sequentially the HD rate. The change of the cross section was found to coincide with the onset of H-induced reconstruction of the Cu(100) surface.

Oxygen abstraction from Cu(111)¹² and Cu(100)¹³ by H(gas) was found to lead to gaseous as well as adsorbed water in two consecutive hydrogenation steps, O(ad) to OH(ad) and OH(ad) to H₂O(ad,gas), which could be successfully interpreted through a sequence of quasi-first-order reaction steps with cross sections σ_O and σ_{OH} . The reactions were observed to accelerate considerably by increasing the temperature.

The present study on the Cu(110) surface was performed in order to investigate whether the D abstraction kinetics is affected by the adsorbate-induced reconstruction of this surface, as was apparent on the Cu(100) surface. Furthermore, measurements of the oxygen abstraction kinetics are intended to complete previous work on the other low-index surfaces and to specify the rate-determining steps as well as the temperature dependence of kinetic phenomena.

2. Experimental Section

The experiments were performed in a UHV chamber equipped with instrumentation for Auger electron spectroscopy, thermal desorption spectroscopy, and reaction kinetics measurements. Two heated tube type (2000 K) atom sources allowed generation of effusive H and D beams. The fluxes delivered by the sources were calculated from the operation parameters, tube temperature and gas throughput, and the H₂/H equilibrium data. As sketched in Figure 1, the H source is located on the axis of a small differentially pumped vacuum chamber (source chamber) which sticks into the main system. On its front end the source chamber exhibits a circular aperture which can be closed by a shutter plate. The ionizer of the quadrupole mass spectrometer located at the source chamber back end has no line-of-sight connection to the entrance aperture which warrants that the signals of the mass spectrometer are proportional to partial pressures due to the randomized flux of particles which enter the source chamber. Through differential pumping these partial pressures are proportional to the rates of formation or desorption of the particles which leave the surface.

The coin-shaped Cu(110) single crystal exhibits two groves and a hole on its side face. Two W wires placed into the groves served for fixing and heating/cooling the crystal. The sample

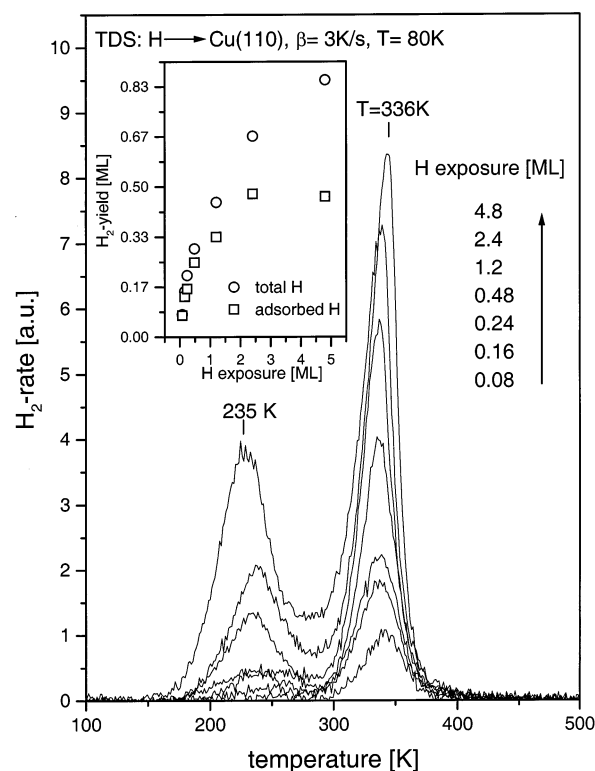


Figure 2. Thermal desorption spectra measured after admitting H to Cu(110) surfaces at 80 K. The H exposure is specified in monolayers, 1 ML = $1.09 \times 10^{15} \text{ cm}^{-2}$. The inset illustrates the total and adsorbed particle uptake at 80 K.

temperature was monitored by a type K thermocouple inserted into the hole and connected to a temperature controller which allowed temperature regulation to a fraction of a degree in the range 80 K to 1100 K. The sample was cleaned by application of sputter/anneal cycles until in Auger spectra no peaks due to contamination were detected.

For measuring the D and O abstraction kinetics, the sample with specific D and O coverages was placed in front of the closed aperture. After opening of the computer-controlled shutter, a defined flux of H atoms was exposed to the surface and reaction products were monitored by multiplexing the quadrupole through masses of interest until reaction completion.

3. Results and Discussion

3.1. Abstraction of D. Thermal desorption spectra measured after admitting increasing H fluences to clean Cu(110) surfaces at 80 K are shown in Figure 2. Two peaks around 235 K (b) and 336 K (s) develop with increasing exposure. The s peak is very similar to the desorption feature from adsorbed H measured after admission of fast H₂ molecules to Cu(110) which are capable of surmounting the activation barrier for adsorption.¹⁴ The two peak structure apparent from Figure 2 was also observed in a study on Cu(110) which utilized H atoms as exposed species¹⁵ and the b peak was tentatively assigned to H absorbed at bulk sites. From the fact that through molecular adsorption the b peak cannot be populated on Cu(110) and similar b features measured at Cu(100)^{16,17} and Cu(111)⁶ surfaces could not be saturated through H admission, it is concluded that the b peak stems from bulk sites. The inset in Figure 2 suggests that saturation of the b peak can also not be achieved on Cu(110), but this feature was not addressed in detail.

Admission of D atoms to Cu(110) surfaces revealed desorption spectra similar to those displayed in Figure 2, with the

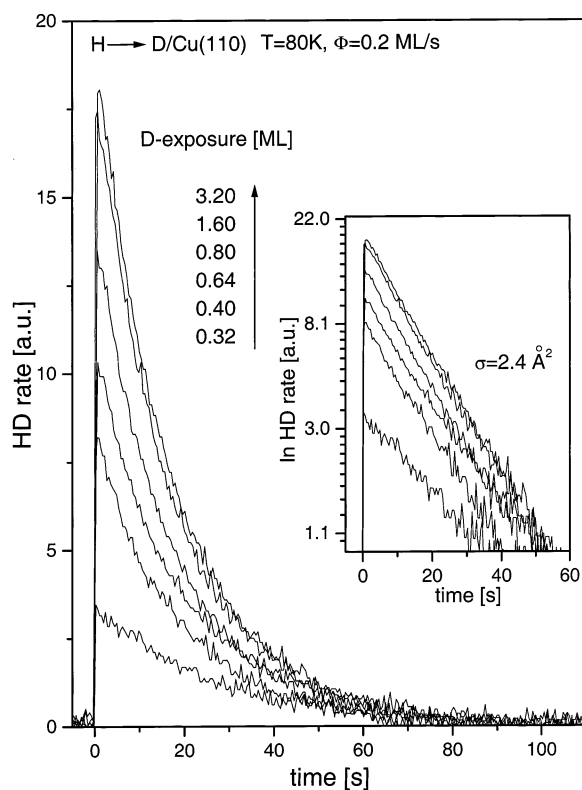


Figure 3. Kinetics of HD measured during admission of H to D-covered Cu(110) surfaces at 80 K. A H flux of 1 ML s⁻¹ corresponds to 1.09×10^{15} H cm⁻² s⁻¹. The inset displays a logarithmic representation of the HD rates.

saturated s peak shifted by 6 K to higher temperatures and an unshifted b peak. That the b peak does not exhibit an isotope shift might be correlated with the reconstruction of the surface by which a smaller isotope effect is suppressed.

The abstraction kinetics measured while admitting a H atom flux of 0.2 ML/s to D-covered Cu(110) surfaces at 80 K are shown in Figure 3. As a common feature of the kinetics at various D precoverages, it is observed that at the start of a reaction the HD rate exhibits a sudden increase to a maximum value followed by a continuous decrease. The inset in Figure 3 illustrates that the rates decay exponentially as a function of the reaction time, as required in a ER reaction scenario. The abstraction cross-section extracted from the HD rates, $\sigma = 2.4$ Å², is similar to the cross-sections obtained at Cu(111), $\sigma = 2.0$ Å², and Cu(100), $\sigma = 2.7$ Å² (late reaction regime). Like on the other two Cu surfaces, on the Cu(110) surface a small fraction of the preadsorbed D, about 1%, gets abstracted into D₂ products.

The kinetics shown in Figure 3 were measured at surfaces which were covered with D at 80 K, i.e., with adsorbed as well as absorbed D. Performing abstraction on surfaces which were preexposed to D at 250 K in order to prevent population of bulk sites did not change the observed kinetics. Postreaction desorption spectra confirmed that D abstraction was complete and removed any adsorbed and absorbed D species from the Cu(110) surface. In contrast to this, on Cu(100) and Cu(111) surfaces absorbed species could not be "abstracted". This might indicate that on Cu(110), exchange between absorbed and adsorbed species is faster than on the other two Cu surfaces.

The characteristics of D abstraction on the three low index Cu surfaces exhibit some face-specific features which indicate a structural aspect in abstraction: reconstruction-related effects are observed on Cu(100), but not on Cu(110), absorbed D atoms

do not get abstracted on Cu(111) and Cu(100), but on Cu(110) they do. However, apart from these details, the Cu surfaces have in common that the kinetics phenomenologies are ER-like, the cross-sections are in the range 2–3 Å², and the contributions of homonuclear D₂ products are very small, only in the 1% range.

A recent DFT calculation of the potential energy surface of H on a Cu(110) surface revealed H binding energies of about 2.3 eV on the most favorable sites, short-bridge, long-bridge, and a pseudo 3-fold site underneath the short bridge.¹⁸ The barriers for H atom movements across the surface were found as only about 0.17 eV. This strong attraction between a Cu(110) surface and incoming H atoms suggests that abstraction is governed by a hot-atom mechanism^{19,20} and the small barriers warrant that hot atoms can easily travel on this surface. This will not change significantly if the surface reconstructs in the missing row structure.²¹ The binding energy of H at the 3-fold hollow sites on Cu(111) is about 2.5 eV¹⁸ and at the 4-fold site on Cu(100) it might be 5% bigger. With respect to the H–Cu binding energy, the three low-index Cu surfaces are similar and the requirement for a hot-atom scenario in abstraction, a strong H–substrate interaction, is fulfilled. However, this alone does not explain why the HD kinetics are ER-like irrespective of the surface orientation (excluding the reconstruction effect on Cu(100)).

As outlined in the Introduction, from the model descriptions, the phenomenology of an ER-like abstraction kinetics is expected in hot-atom reactions if the probabilities for reaction and sticking of hot atoms are similar, $p_r/p_s = 1$. In view of the results on Ni(110)⁴ and Pt(111),⁵ where the abstraction kinetics are indicative of efficient sticking of hot atoms, one might ask why on Cu surfaces hot atom sticking is inefficient.

Sticking of hot atoms requires some energy transfer from the hot atom to the substrate. Substrate phonon excitation is inefficient due to the large mass-mismatch between H and a metal atom and energy-consuming collisions of hot H atoms with preadsorbed D species are rare at small D coverages. Therefore, it is assumed that this energy transfer can only be provided by electronic excitation, of which the electron–hole excitation mechanism appears as the most probable mechanism. Comparing the electronic densities of states at the Fermi level of Pt, Ni, and Cu, it is observed that these densities decrease from Pt over Ni to Cu. The same trend was observed for the efficiency of hot-atom sticking. If hot-atom sticking is mediated by electron–hole excitations, it is no surprise that on a Cu(110) surface it is not efficient and that the other Cu surfaces exhibit the same feature. Whether the electronic density of states at the Fermi level and the kinetics phenomenology of an abstraction reaction are in fact related can be tested with Ag, which exhibits a small electron density of states at the Fermi level. Inefficient hot-atom sticking therefore should cause the HD kinetics in D abstraction by H to exhibit ER-like phenomenology. Experiments on Ag(100) confirmed this expectation.²²

3.2. Abstraction of O. In previous studies of abstraction of O on Cu(111)¹³ and Cu(100)¹⁴ surfaces it was observed that at temperatures below the water desorption temperature gaseous as well as adsorbed water were reaction products. To select the appropriate reaction temperatures for abstraction measurements, thermal desorption spectra were measured of water and O(ad)/water adsorbed on Cu(110). Figure 4 illustrates that water desorbs molecularly around 165 K and that coadsorbed oxygen modifies the strength of the water–Cu(110) interaction. The data in Figure 4 are in excellent agreement with earlier work²³ in which in addition to the desorption features seen in Figure

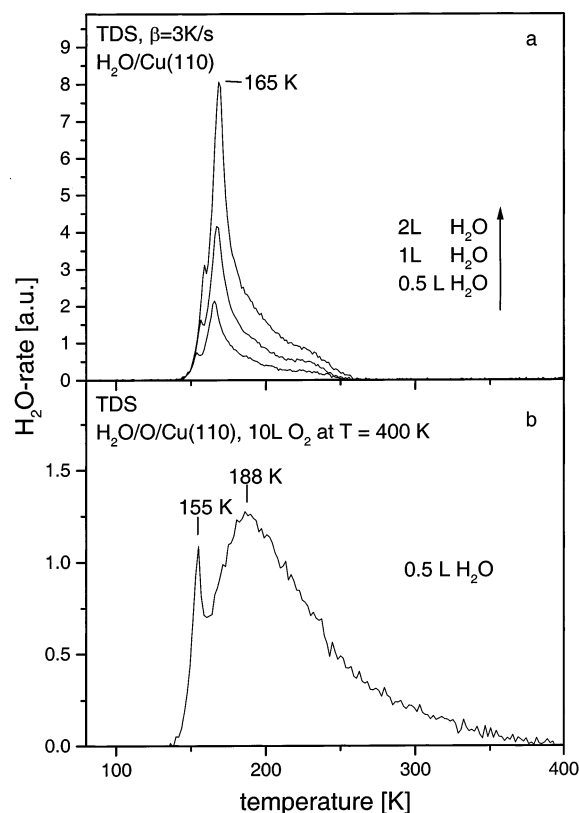


Figure 4. Thermal desorption spectra of water on Cu(110) (a), and oxygen-covered Cu(110) surfaces (b).

4b at low water coverages on oxygen precovered Cu(110) a water peak due to OH/OH disproportionation at 285 K was reported.

The desorption temperatures apparent from Figure 4 suggest that at reaction temperatures below 140 K thermal desorption of water formed through interaction of adsorbed O with gaseous H can be neglected. Accordingly, gaseous water products monitored during reaction below 140 K should stem from desorption events induced by the exothermicity of the reaction which amounts to about 5 eV, taking the oxygen adsorption energy and water enthalpy of formation into account. Between 150 and 250 K, isothermal desorption of water should occur with increasing rate. Above 250 K, the thermal desorption step is so fast that it is not rate limiting and any water formed should desorb immediately into the gas phase.

The kinetics of water measured during admission of H to Cu(110) surfaces on which O adlayers were prepared by a 10 L oxygen dose at 400 K are displayed in Figure 5. Irrespective of the temperature, the water rates have in common that they initially increase linearly from zero, which is required for the rate of water formed through two consecutive reactions with $\text{OH}(\text{ad})$ as intermediate, $\text{H} + \text{O}(\text{ad}) \rightarrow \text{OH}(\text{ad})$, $\text{H} + \text{OH}(\text{ad}) \rightarrow \text{H}_2\text{O}(\text{ad, gas})$. The fact that even at 100 K, 60 K below its desorption temperature, water was observed in the gas phase illustrates that the significant exothermicity of the reaction leads to spontaneous ejection of the product into the gas phase. However, as seen from the water yields shown in the inset of Figure 5, at 100 K reaction temperature the amount of water recovered in post-reaction thermal desorption spectra is twice the amount ejected into the gas phase during reaction. These features are very similar to those observed on Cu(100) and Cu(111).

At reaction temperatures of 150 and 200 K, the gaseous water rates exhibit second local maxima at late reaction times which

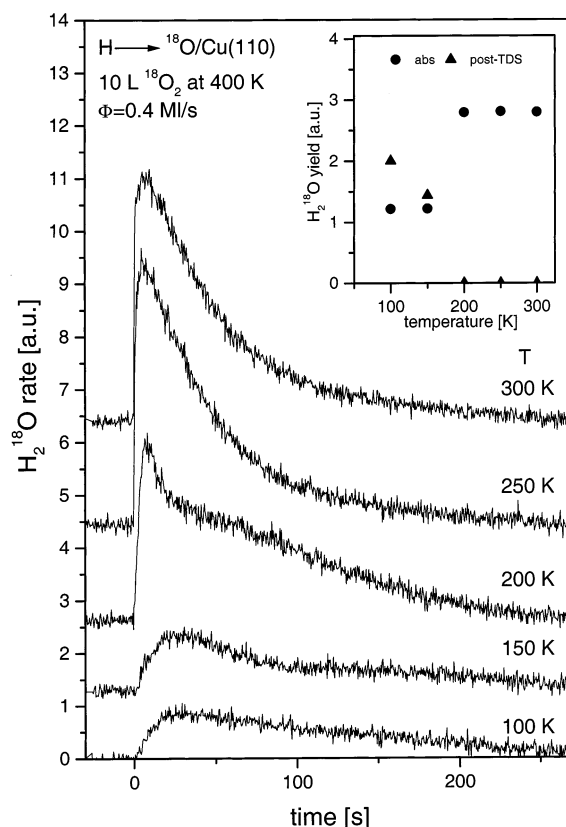


Figure 5. Kinetics of water formation measured during admitting a H flux to oxygen-covered surfaces at various temperatures. The oxygen adlayers were prepared by exposing 10 L of oxygen at 400 K. The inset displays the amount of water collected during reaction (circles) and in post-reaction TDS (triangles).

illustrate the operation of slow isothermal desorption, as discussed above. At 250 and 300 K, the water rate initially increases linearly and exhibits an exponential decay after the rate maximum. This is in accordance with the kinetics of a two-step reaction which is controlled by the slow step at late reaction times.

Ideally, the yields of gaseous and adsorbed water products should add to a constant value, since all preadsorbed oxygen was reacted to water during H admission. It is seen in Figure 5 that the sum of the yields at 150 K is smaller than that at lower and higher temperatures. The reason for this is a loss of products through isothermal desorption of water between reaction completion and recording the thermal desorption spectrum. At and above 200 K, isothermal desorption is so fast that adsorbed products do not exist any more on the time scale of the experiment. Within experimental error, the total water yield at these temperatures is the same as at 100 K, as it should be without interference of isothermal desorption.

From the temperature-dependent kinetics shown in Figure 5, one cannot decide whether hydrogenation of $\text{O}(\text{ad})$ or $\text{OH}(\text{ad})$ is the rate-limiting slow step. To identify the slower step, H was admitted to oxygen adlayers at 100 K for limited amounts of time and subsequently TD spectra were recorded to check for the occurrence of water. The series of spectra obtained in this way are shown in Figure 6. Two peaks are apparent from these data: one at 165 K, which corresponds to the adsorbed final water product, and one at 240 K, which must stem from a reaction of the intermediate OH group. Since $\text{OH}(\text{ad}) + \text{OH}(\text{ad})$ disproportionation occurs at 285 K,²³ and water desorption from oxygen precovered surfaces around 188 K, see Figure 4, the only origin of the water peak at 240 K can be $\text{OH}(\text{ad}) +$

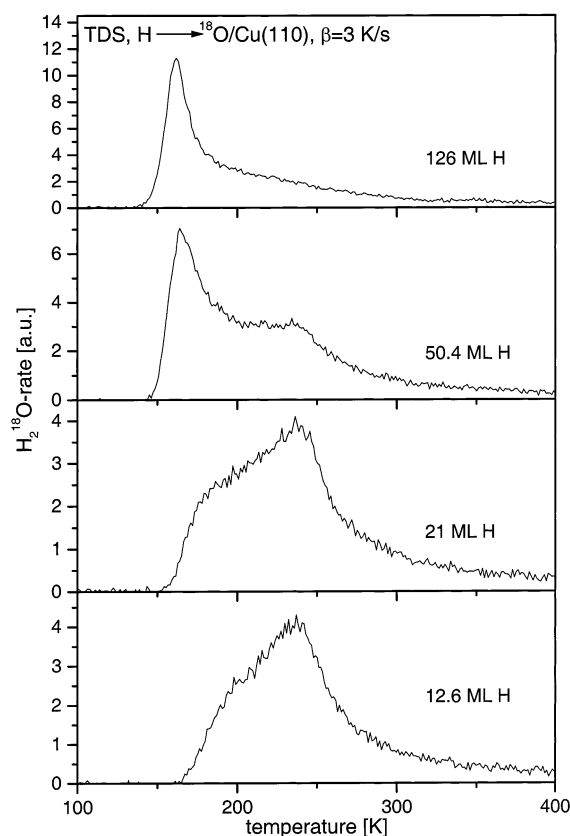


Figure 6. Thermal desorption spectra measured after admitting increasing fluences of H to oxygen-covered Cu(110) surfaces at 100 K.

H(ad) recombination. The constant peak temperature qualifies this reaction as of first order, which is in line with the fact that the coverage of H(ad) is sufficiently high and not rate limiting for recombination of OH(ad) and H(ad). The existence of measurable quantities of OH(ad) on the surface allows us to conclude that hydrogenation of O(ad) to OH(ad) is the fast step and OH(ad) hydrogenation is the slow step. If the opposite were true, it would be impossible to monitor any surface reaction between OH(ad) and H(ad) and one would only observe a peak around 165 K due to the final adsorbed water product.

From the study of the water reaction on Cu(111) surfaces,¹³ it was concluded that hydrogenation of O with a cross section of $\sigma_O = 0.26 \text{ \AA}^2$ is the slow step and hydrogenation of OH with a cross-section of $\sigma_{OH} = 5.8 \text{ \AA}^2$ is the fast step. The study of oxygen abstraction on Cu(100) surfaces revealed that O hydrogenation is the slow step and OH hydrogenation is the fast step, but cross sections were not determined.

If isothermal desorption can be neglected, the water kinetics can be used to determine the cross section of the slow step. The product rate $R(t)$ of the two consecutive reaction steps is a sum of two exponentials, $R(t) \propto \exp(-\sigma_O \phi t) - \exp(-\sigma_{OH} \phi t)$, and the smaller cross-section determines $R(t)$ late in the reaction. To exclude coverage and structural effects hidden in a measured rate, the kinetics were determined at various coverages prior to extraction of a cross-section. Figure 7 shows the water kinetics at 300 K where desorption limitation is negligible for several oxygen coverages. The logarithmic water rates displayed in the inset exhibit the same slope and the extraction of a cross-section is justified. A cross-section of $\sigma_O = 0.6 \text{ \AA}^2$ was determined from the kinetics in Figure 7.

Abstraction of oxygen toward water on other surfaces than of Cu were investigated on Ru(001),²⁴ Ni(100),²⁵ Ir(111),²⁶ and

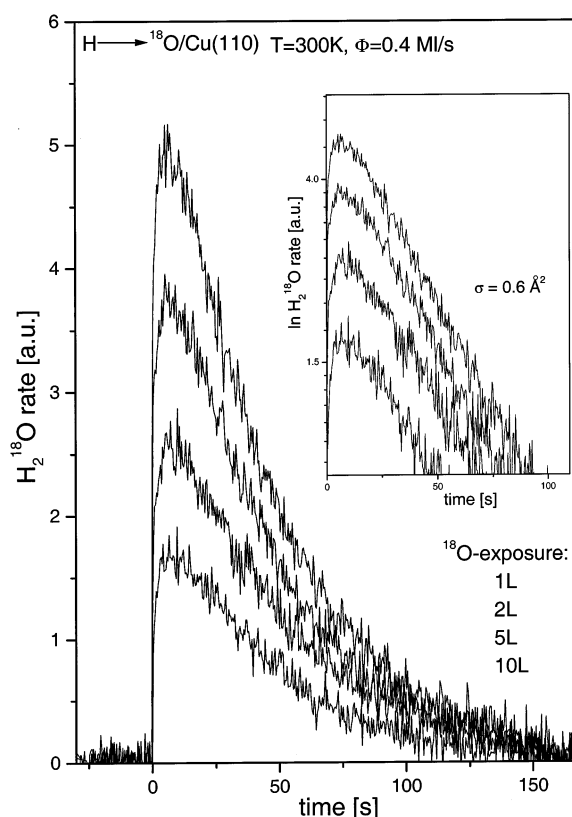


Figure 7. Kinetics of water formation at various initial oxygen precoverages measured during admission of H atoms at 300 K. The inset provides a logarithmic representation of the rates.

Pt(111)²⁷ surfaces. On Pt(111), the hydrogenation of surface hydroxyl was found as rate limiting, on the other surfaces hydrogenation of oxygen was reported as the slow step. The cross-sections of the slow step were determined on these metals as several tenths of an \AA^2 . These rather small cross-sections indicate that the slow step is geometrically difficult. Depending on the actual adsorption site of O(ad) or OH(ad), either hydrogenation step could exhibit this feature and the slow step would not be a characteristic of a particular element, e.g., Cu or Pt. It is improbable that the exothermicity determines whether a step is fast or slow, because then in general the first hydrogenation step, $\text{O(ad)} \rightarrow \text{OH(ad)}$, would be the slow step: the overall exothermicity of the two-step reaction originates primarily from the second hydrogenation step since OH is much more strongly bound to a metal surface than water.

The assumption that geometrical O- and OH-adsorption site-related effects control whether hydrogenation of O or of OH is rate-determining might explain why in the water formation reactions from adsorbed O and gaseous H investigated so far, on Ni, Pt, Cu, Ir, and Ru, no simple rule is apparent which would allow us to predict their speed hierarchy. More studies are needed to clarify this aspect.

4. Conclusions

The kinetics of the reactions of gaseous H atoms with D and O adsorbed on Cu(110) surfaces was measured and compared with the kinetics of these reactions on Cu(100) and Cu(111) and other metal surfaces. Although a hot-atom process, the HD kinetics of the $\text{H} \rightarrow \text{D(ad)}$ abstraction reaction exhibits an Eley-Rideal (ER) kinetics phenomenology with a cross-section of 2.4 \AA^2 , and only a very small contribution of D_2 products was observed. As origin of the ER phenomenology in D by H

abstraction on Cu surfaces, it is proposed that sticking of hot atoms on Cu mediated by electron–hole excitations is inefficient due to the small density of states at the Fermi level. The reaction of H with O on Cu(110) leads to adsorbed and gaseous water at 100 K, as on the other two low index surfaces of Cu and other metals. Well above the water desorption temperature, only gaseous water was observed. Water is formed on Cu(110) in a sequence of two hydrogenation steps, O(ad) to OH(ad) and OH(ad) to H₂O(ad, gas), of which the latter is rate-determining with a cross-section of 0.6 Å². From a comparison of these results with those on other metal surfaces, it is concluded that geometrical effects regulate which one of the hydrogenation reactions is rate-determining.

References and Notes

- (1) Rettner, C. T. *J. Chem. Phys.* **1994**, *101*, 1529.
- (2) Rettner, C. T.; Auerbach, D. J. *J. Chem. Phys.* **1996**, *104*, 2732.
- (3) Eilmsteiner, G.; Walkner, W.; Winkler, A. *Surf. Sci.* **1996**, *352*, 263.
- (4) Kammler, Th.; Lee, J.; Küppers, J. *J. Chem. Phys.* **1997**, *106*, 7362.
- (5) Wehner, S.; Küppers, J. *J. Chem. Phys.* **1998**, *108*, 3353.
- (6) Kammler, Th.; Küppers, J. *J. Chem. Phys.* **1999**, *111*, 8115.
- (7) Dinger, A.; Lutterloh, C.; Küppers, J. *Chem. Phys. Lett.* **1999**, *311*, 202.
- (8) Kammler, Th.; Wehner, S.; Küppers, J. *J. Chem. Phys.* **1998**, *109*, 4071.
- (9) Kammler, Th.; Kolovos-Vellianitis, D.; Küppers, J. *Surf. Sci.* **2000**, *460*, 91.
- (10) Jackson, B.; Sha, X.; Guvenc, Z. B. *J. Chem. Phys.* **2002**, *116*, 2599.
- (11) Harris, J.; Kasemo, B. *Surf. Sci.* **1981**, *105*, L281.
- (12) Kammler, Th.; Küppers, J. *J. Phys. Chem. B* **2001**, *105*, 8369.
- (13) Kolovos-Vellianitis, D.; Kammler, Th.; Küppers, J. *Surf. Sci.* **2001**, *482–485*, 166.
- (14) Anger, G.; Winkler, A.; Rendulic, K. D. *Surf. Sci.* **1989**, *220*, 1.
- (15) Sandl, P.; Bischler, U.; Bertel, E. *Surf. Sci.* **1993**, *291*, 29.
- (16) Chorkendorff, I.; Rasmussen, P. B. *Surf. Sci.* **1991**, *248*, 35.
- (17) Kolovos-Vellianitis, D.; Kammler, Th.; Küppers, J. *Surf. Sci.* **2000**, *454–456*, 316.
- (18) Bae, C.; Freeman, D. L.; Doll, J. D.; Kresse, G.; Hafner, J. *J. Chem. Phys.* **2000**, *113*, 6926.
- (19) Wehner, S.; Küppers, J. *J. Chem. Phys.* **1998**, *109*, 294.
- (20) Jackson, B.; Lemoine, D. *J. Chem. Phys.* **2001**, *114*, 474.
- (21) Hayden, B. E.; Lackey, D.; Schott, J. *Surf. Sci.* **1990**, *239*, 119.
- (22) Kolovos-Vellianitis, D.; Küppers, J. To be published.
- (23) Bange, K.; Grider, D. E.; Madey, T. E.; Sass, J. K. *Surf. Sci.* **1984**, *136*, 38.
- (24) Schick, M.; Xie, J.; Mitchell, W. J.; Weinberg, W. H. *J. Chem. Phys.* **1996**, *104*, 7713.
- (25) Kammler, T.; Scherl, M.; Küppers, J. *Surf. Sci.* **1997**, *382*, 116.
- (26) Hagedorn, C. J.; Weiss, M. J.; Weinberg, W. H. *J. Vac. Sci. Technol. A* **2000**, *18*, 1497.
- (27) Biener, J.; Lang, E.; Lutterloh, C.; Küppers, J. *J. Chem. Phys.* **2002**, *116*, 3063.